Contents

1. Overview

The CP-even fraction $F_+^{4\pi}$ of 4π can be determined through the evaluation of

$$M_i^{K_S^0\pi\pi} = h_{K_S^0\pi\pi}(T_i^{K_S^0\pi\pi} + T_{-i}^{K_S^0\pi\pi} - 2\,c_i\sqrt{T_i^{K_S^0\pi\pi}T_{-i}^{K_S^0\pi\pi}}\,(2F_+^{4\pi}-1)) \qquad (1.1)$$

and

$$M_i^{K_L^0\pi\pi} = h_{K_L^0\pi\pi}(T_i^{K_L^0\pi\pi} + T_{-i}^{K_L^0\pi\pi} + 2\,c_i'\sqrt{T_i^{K_L^0\pi\pi}T_{-i}^{K_L^0\pi\pi}}\,(2F_+^{4\pi}-1)) \qquad (1.2)$$

where the M_i denote the number of events in bin i of the $K_S^0\pi\pi$/ $K_L^0\pi\pi$ Dalitz-Plot tagged against 4π, the T_i the relative amount of events in bin i of flavour-tagged $K_S^0\pi\pi$/ $K_L^0\pi\pi$ Dalitz-Plot and the h are normalisation factors.

By summing over the bins i and $-i$ these expressions become

$$MM_i^{K_S^0\pi\pi} = M_i^{K_S^0\pi\pi} + M_i^{K_S^0\pi\pi} = 2{\cdot}h_{K_S^0\pi\pi}(T_i^{K_S^0\pi\pi} + T_{-i}^{K_S^0\pi\pi} - 2\,c_i\sqrt{T_i^{K_S^0\pi\pi}T_{-i}^{K_S^0\pi\pi}}\,(2F_+^{4\pi}-1))$$
$$(1.3)$$

and

$$MM_i^{K_L^0\pi\pi} = M_i^{K_L^0\pi\pi} + M_{-i}^{K_L^0\pi\pi} = 2{\cdot}h_{K_L^0\pi\pi}(T_i^{K_L^0\pi\pi} + T_{-i}^{K_L^0\pi\pi} + 2\,c_i'\sqrt{T_i^{K_L^0\pi\pi}T_{-i}^{K_L^0\pi\pi}}\,(2F_+^{4\pi}-1))$$
$$(1.4)$$

The following report summarised how the values for $MM_i^{K_S^0\pi\pi}$ and $MM_i^{K_L^0\pi\pi}$ are determined.

2. Binned $K_S^0\pi\pi$ vs 4π yields

2.1 Overview

The values for MM_i are obtained using:

$$MM_i = (N_i^{meas} - B_i^{peak} - B_i^{flat})/\epsilon_i \tag{2.1}$$

MM_i : absolute number of 4π vs $K_S^0\pi\pi$ events in bin i. This is the quantity that enters the fit for F_+.

N_i^{meas} : total number of reconstructed and selected events in bin i.

B_i^{peak} : number of reconstructed and selected peaking bkg. events in bin i. The only peaking bkg. expected is $K_S^0\pi\pi$ vs $K_S^0\pi\pi$.

B_i^{flat} : number of reconstructed and selected flat bkg. events in bin i.

ϵ_i : reconstruction and selection efficiency for 4π vs $K_S^0\pi\pi$ events in bin i.

2.2 Raw number of selected 4π vs $K_S^0\pi\pi$ events

The selection of 4π vs $K_S^0\pi\pi$ was done as outlined in Chris' report. The resulting numbers are listed below.

bin i	$N_i^{meas} \pm \sqrt{N_i^{meas}}$
1	38 ± 6.16
2	22 ± 4.69
3	21 ± 4.58
4	12 ± 3.46
5	59 ± 7.68
6	24 ± 4.90
7	30 ± 5.48
8	42 ± 6.48

Table 2.1: *Number N_i^{meas} of reconstructed 4π vs $K_S^0\pi\pi$ events summed over bin i and -i. The errors are taken as $\sqrt{N_i^{meas}}$.*

2.3 Determination of number of peaking background events

It is assumed that the only peaking bkg to $K_S^0 \pi \pi$ vs 4π is $K_S^0 \pi \pi$ vs $K_S^0 \pi \pi$.
The number of peaking bkg events in bin i B_i^{peak} is determined from

$$B_i^{peak} = B_{tot}^{peak} \cdot a_i^{peak} \qquad (2.2)$$

where B_{tot}^{peak} denotes the total number of $K_S^0 \pi \pi$ vs $K_S^0 \pi \pi$ events in the selected data sample and a_i^{peak} the percentage of $K_S^0 \pi \pi$ vs $K_S^0 \pi \pi$ events in bin i.

2.3.1 Total number of peaking background events in selected data sample

The total number of peaking bkg events in the selected sample is determined using the generic MC. The same reconstruction and selection as to the data is applied to the generic MC. This results in 60 and 243 selected $K_S^0 \pi \pi$ vs $K_S^0 \pi \pi$ events in the lumix10 and lumix20 sample respectively.

$$B_{tot}^{peak} = 18.45 \qquad (2.3)$$

2.3.2 Peaking background events per bin

Since the generic MC has been generated without taking into account the quantum correlations and no model-dependence should be introduced to the analysis, the relative amount of peaking bkg events per bin has to be determined with data.
Therefore the CLEO data is reconstructed and selected in the same way as for the signal decay, apart from a 'reversed K_S^0 veto'. This means that instead of rejecting events where two of the pions from the 4π have a K_S^0 flight significance >0, events with a K_S^0 flight significance >2 are selected to ensure a reasonably clean $K_S^0 \pi \pi$ vs $K_S^0 \pi \pi$ sample.
Unfortunately 'reversed K_S^0 veto' introduced a bias in the distribution of expected $K_S^0 \pi \pi$ vs $K_S^0 \pi \pi$ events over the bins. Figure 2.1 shows the distribution of $K_S^0 \pi \pi$ vs $K_S^0 \pi \pi$ events over the bins for the selection with the K_S^0-Veto and the 'reversed K_S^0 veto' on $K_S^0 \pi \pi$ vs $K_S^0 \pi \pi$ signal MC.
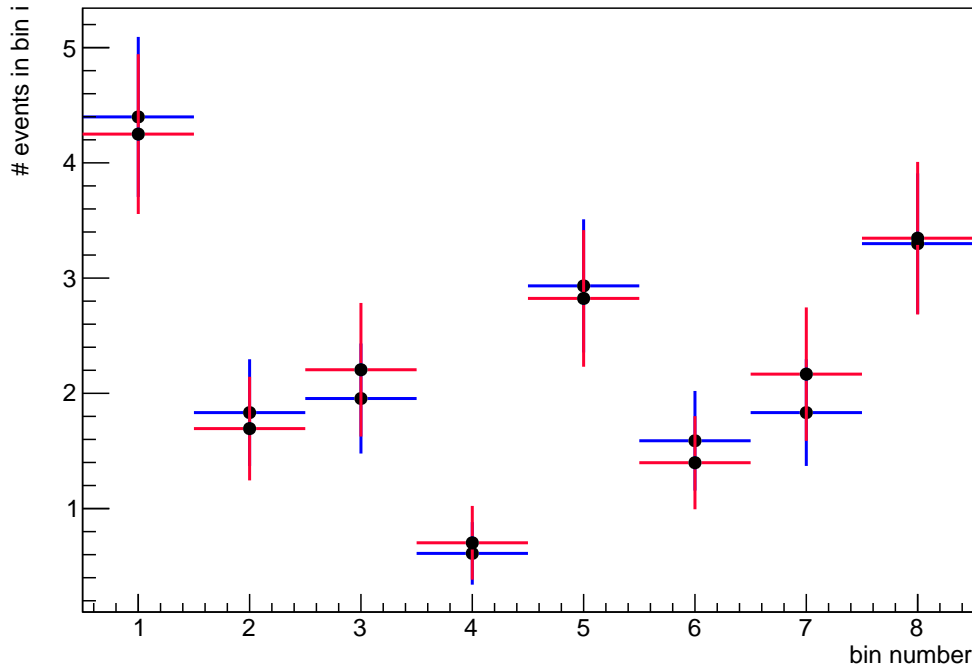
Figure 2.1: *Distribution of $K_S^0\pi\pi$ vs $K_S^0\pi\pi$ events over the bins determined by using $K_S^0\pi\pi$ vs $K_S^0\pi\pi$ MC. Blue: reversed K_S^0 veto cut of FS>2, red: K_S^0 veto cut of FS<0 as is used in the data sample.*

To compensate for this bias the values for the percentage of $K_S^0\pi\pi$ vs $K_S^0\pi\pi$ per bins obtained from the data are being weighted with the ratio of reversed K_S^0 veto over the K_S^0 veto efficiencies determined from the $K_S^0\pi\pi$ vs $K_S^0\pi\pi$ signal MC sample. This yields the total amount of $K_S^0\pi\pi$ vs $K_S^0\pi\pi$ contamination in the data sample listed below.

bin i	B_i^{peak}
1	$4.21854 \pm 2 \oplus 0.637882$
2	$1.68165 \pm 1.5 \oplus 0.434214$
3	$2.18858 \pm 1.5 \oplus 0.559566$
4	$0.697849 \pm 0.5 \oplus 0.314724$
5	$2.80305 \pm 1.5 \oplus 0.562877$
6	$1.38776 \pm 1.5 \oplus 0.391982$
7	$2.15081 \pm 1.5 \oplus 0.559324$
8	$3.32175 \pm 1.5 \oplus 0.624964$

Table 2.2: *Number of peaking background events per bin in the data sample. The first error is the Poisson error on the yields, the second error comes from the systematic uncertainty on the distribution over the bins.*

2.3.2.1   Cleanness of $K_S^0 \pi\pi$ vs $K_S^0 \pi\pi$ sample

The gen MC suggest that the 'reversed K_S^0 veto' yields a sample of 96% $K_S^0 \pi\pi$ vs $K_S^0 \pi\pi$ events. The rest is distributed as follows:

- 2.8% 4π vs $K_S^0 \pi\pi$

- 0.2% flat

- 1.0% $K_S^0 \pi\pi$ vs $K_S^0 K_S^0$ (with the $K_S^0 K_S^0$ on the $K_S^0 \pi\pi$ side)

This will be accounted for in the systematic uncertainties in Section 4.1.2.2.

2.4   Determination of number of flat background events

The number of flat bkg events is determined using the usual sidebands (denoted A, B, C and D). The number of events in the sidebands is extrapolated to give the amount of flat bkg in the signal region using the equation

$$B_{tot}^{flat} = \frac{a_S}{a_D} N_D + \sum_{j=A,B,C} \frac{a_S}{a_j} (N_j - \frac{a_j}{a_D} N_D) \tag{2.4}$$

where N_j is the number of events in sideband j, a_j is the area of sideband j and a_S is the area of the signal region. The results are listed below (no errors are assumed on the values of a_j).

N_A	1
N_B	0
N_C	20
N_D	2
B_{tot}^{flat}	11.64

Table 2.3: *Number of flat bkg in the sideband and extrapolated to the signal region.*

To get the number of flat bkg events in bin i, the relative area of bin i is determined using the `dkpp_babar.root` histogram. Assuming no error on the relative area of bin i the number of flat bkg events are:

bins	number of flat bkg events
1	3.85 ± 2
2	1.33 ± 1
3	0.74 ± 1
4	0.69 ± 0.5
5	1.55 ± 1.5
6	0.94 ± 1
7	0.98 ± 1
8	1.56 ± 1.5

Table 2.4: *Number of flat bkg events per bin.*

2.5 Determination of the signal selection-efficiency

The signal selection efficiency in each bin is determined using a sample of 266998 $K_\mathrm{S}^0 \pi\pi$ vs 4π signal MC events.

bin	ϵ
1	0.1553 ± 0.0012
2	0.1529 ± 0.0021
3	0.1761 ± 0.0029
4	0.1671 ± 0.0030
5	0.1583 ± 0.0019
6	0.1642 ± 0.0025
7	0.1551 ± 0.0024
8	0.1607 ± 0.0020

Table 2.5: *Signal efficiency per bin.*

2.6   Bkg substracted, efficiency corrected, rescaled signal yields

bin	MM_i
1	$30.7804 \pm 6.97383 \oplus 0.241629 \oplus 0.655893$
2	$19.8284 \pm 5.24652 \oplus 0.26636 \oplus 0.453361$
3	$16.3846 \pm 4.46561 \oplus 0.273724 \oplus 0.50743$
4	$10.1474 \pm 3.37991 \oplus 0.180279 \oplus 0.300871$
5	$55.1394 \pm 8.04054 \oplus 0.676977 \oplus 0.567952$
6	$21.0775 \pm 5.07712 \oplus 0.325249 \oplus 0.381242$
7	$27.6736 \pm 5.93899 \oplus 0.432454 \oplus 0.576076$
8	$36.8818 \pm 6.77579 \oplus 0.448323 \oplus 0.620996$

Table 2.6: *$M_i + M_{-i}$ The first error is the Poisson error on the raw data yields and the bkg yields, the second error comes from the limited data and MC samples used to determine the distribution of peaking bkg events and the third from the signal efficiency.*

2.7   Summary

bin	raw yields	B_i^{peak}	B_i^{flat}	signal
1	38	4.219	3.846	30.78
2	22	1.682	1.327	19.83
3	21	2.189	0.7433	16.38
4	12	0.6978	0.6875	10.15
5	59	2.803	1.55	55.14
6	24	1.388	0.941	21.08
7	30	2.151	0.9804	27.67
8	42	3.322	1.561	36.88

Table 2.7: *Summary of contributions to the raw yields per bin.*

3. Binned $K_L^0 \pi\pi$ vs 4π yields

3.1 Overview

The values for MM_i are obtained using:

$$MM_i = (N_i^{meas} - B_i^{peak} - B_i^{flat} - B_i^{cont})/\epsilon_i \qquad (3.1)$$

MM_i : absolute number of 4π vs $K_L^0 \pi\pi$ events in bin i. This is the quantity that enters the fit for F_+.

N_i^{meas} : total number of reconstructed and selected events in bin i.

B_i^{peak} : number of reconstructed and selected peaking bkg. events in bin i.

B_i^{flat} : number of reconstructed and selected flat bkg. events in bin i.

B_i^{cont} : number of reconstructed and selected continuum bkg. events in bin i.

ϵ_i : reconstruction and selection efficiency for 4π vs $K_L^0 \pi\pi$ events in bin i.

3.2 Raw number of selected 4π vs $K_L^0 \pi\pi$ events

The selection of 4π vs $K_L^0 \pi\pi$ was done as outlined in Chris' report. The resulting numbers are listed below.

bin i	$N_i^{meas} \pm \sqrt{N_i^{meas}}$
1	172 ± 13.11
2	71 ± 8.43
3	60 ± 7.75
4	25 ± 5
5	59 ± 7.68
6	32 ± 5.66
7	71 ± 8.43
8	99 ± 9.95

Table 3.1: *Number N_i^{meas} of reconstructed 4π vs $K_L^0 \pi\pi$ events summed over bin i and -i. The errors are taken as $\sqrt{N_i^{meas}}$.*

3.3   Determination of number of peaking background events

Three decays are identified as peaking bkg (peaking in missing mass squared) for $K_L^0\pi\pi$ vs 4π using the gen MC (see Figure 3.1):

- $K_L^0\pi\pi$ vs $K_S^0\pi\pi$: 8% of the events in the signal window

- $K_S^0\pi\pi$ vs 4π: 1.9% of the events in the signal window

- $K_S^0\pi\pi$ vs $K_S^0\pi\pi$: 0.3% of the events in the signal window

(signal window: $0.2\,GeV^2 <$ miss. mass sq $< 0.3\,GeV^2$). Due to the very low contribution the $K_S^0\pi\pi$ vs $K_S^0\pi\pi$ bkg is being neglected.
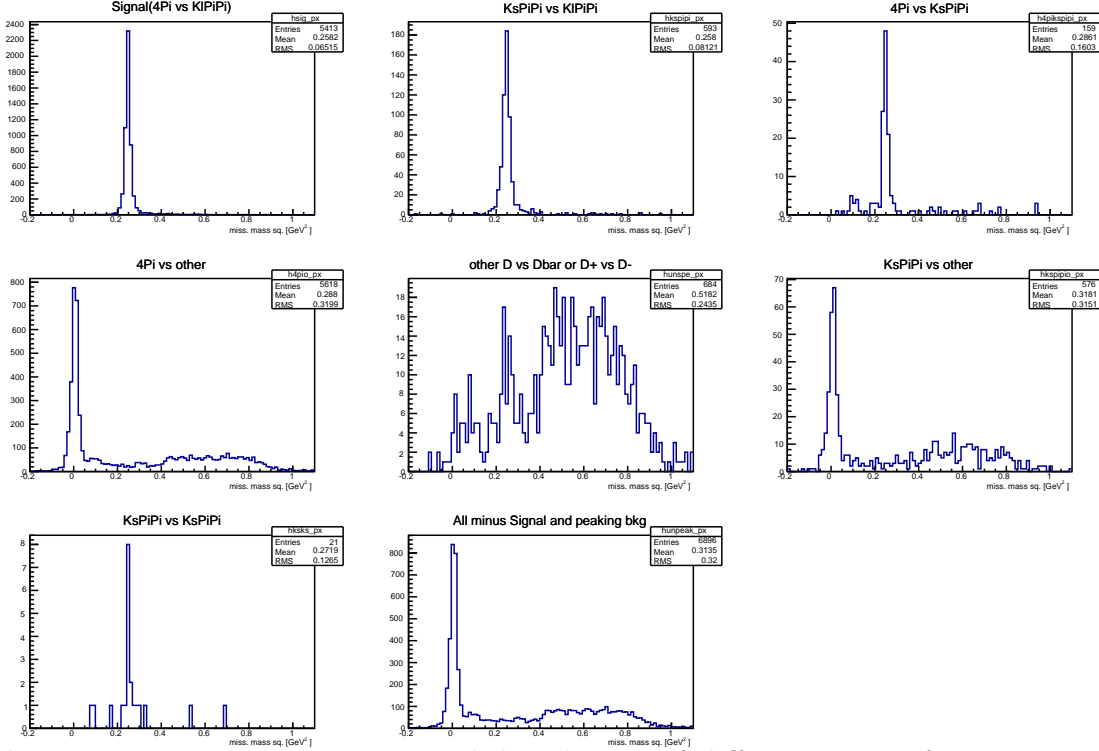
Figure 3.1: *Missing mass squared distribution of different types of events reconstructed as $K_L^0\pi\pi$ vs 4π according to the gen MC.*

As for the $K_S^0\pi\pi$ vs 4π the number of peaking bkg events per bin is determined from

$$B_i^{peak} = B_{tot}^{peak} \cdot a_i^{peak} \tag{3.2}$$

for both bkgs separately, where B_{tot}^{peak} denotes the total number of peaking bkg events in the selected data sample and a_i^{peak} the percentage of peaking bkg events in bin i.

3.3.1 Total number of peaking background events in selected data sample

The total number of peaking bkg events in the selected sample is determined using the generic MC. The same reconstruction and selection as to the data is applied to the generic MC. This results in 98 ± 9.90 and 419 ± 20.47 selected $K_L^0\pi\pi$ vs $K_S^0\pi\pi$ events in the lumix10 and lumix20 sample respectively and 15 ± 3.87 and 90 ± 9.49 $K_S^0\pi\pi$ vs 4π events (the errors are taken to be the sqrt of the yields). These numbers are then scaled appropriately to give the expected number of total bkg events in the reconstructed data sample and no error on the scaling factors is assumed.

$$B_{tot}^{peak}(K_L^0\pi\pi \, vs \, K_S^0\pi\pi) = 35.51 \tag{3.3}$$

and

$$B_{tot}^{peak}(K_S^0\pi\pi \, vs \, 4\pi) = 9.42 \tag{3.4}$$

Since the branching fraction of $D \to K_L^0\pi\pi$ is unknown, the fraction of $K_L^0\pi\pi$ events in the gen MC sample can't be completely accurate. This will be accounted for by applying a systematic to the number of events obtained from the gen MC (by assuming that the branching fraction used by CLEO is 20% too small/big).

3.3.2 Distribution of $K_L^0\pi\pi$ vs $K_S^0\pi\pi$ background events over bins

As for the $K_S^0\pi\pi$ vs $K_S^0\pi\pi$ bkg in $K_S^0\pi\pi$ vs 4π the distribution of $K_L^0\pi\pi$ vs $K_S^0\pi\pi$ events per bin is determined by applying a 'reversed K_S^0 veto' on the data. The gen MC sample suggests that after the reversed K_S^0 veto sample contains:

- $K_L^0\pi\pi$ vs $K_S^0\pi\pi$: 92%

- flat events: 5%

- $K_L^0\pi\pi$ vs 4π: 1.5%

- $K_S^0\pi\pi$ vs $K_S^0\pi\pi$: 1.5%

The last two are neglected for now (a systematic will be appointed later).

In order to obtain the distribution of $K_L^0\pi\pi$ vs $K_S^0\pi\pi$ events over the bins, the contribution of flat bkg events is estimated as in Section 2.4 and removed from the data.

3.3.2.1 Selection-bias

Unfortunately 'reversed K_S^0 veto' introduced a bias in the distribution of expected $K_L^0\pi\pi$ vs $K_S^0\pi\pi$ events over the bins.
To compensate for this bias the values for a_i^{peak} are being weighted with the ratio of reversed K_S^0 veto over the K_S^0 veto efficiencies determined from the $K_L^0\pi\pi$ vs $K_S^0\pi\pi$ signal MC sample.

3.3.3 Distribution of $K_S^0\pi\pi$ vs 4π background events over bins

The 'true' distribution of $K_S^0\pi\pi$ vs 4π events in phasespace is taken from the results of the $K_S^0\pi\pi$ vs 4π analysis, namely the values of Table 2.6.

3.3.4 Resulting number of peaking background events in selected data sample

Applying these scaling values to the factors a_i yields the total amount of peaking bkg contamination in the data sample listed below.

bin i	$B_i^{peak}(K_L^0\pi\pi\, vs\, K_S^0\pi\pi)$
1	$12.267 \pm 3.5 \oplus 1.06294$
2	$3.81339 \pm 2 \oplus 0.666631$
3	$2.85437 \pm 2 \oplus 0.608983$
4	$1.48931 \pm 1.5 \oplus 0.442086$
5	$3.68781 \pm 2 \oplus 0.63337$
6	$1.72474 \pm 1.5 \oplus 0.415589$
7	$4.03395 \pm 2 \oplus 0.709566$
8	$5.63443 \pm 2.5 \oplus 0.804392$

Table 3.2: *Number of $K_S^0\pi\pi$ vs $K_L^0\pi\pi$ background events per bin in the data sample. The first error is the Poisson error on the yields, the second error comes from the sys- tematic uncertainty on the distribution over the bins.*

bin i	$B_i^{peak}(K_S^0\pi\pi\, vs\, 4\pi)$
1	$1.32987 \pm 1 \oplus 0.302816$
2	$0.856693 \pm 1 \oplus 0.227813$
3	$0.707903 \pm 0.5 \oplus 0.194539$
4	$0.438423 \pm 0.5 \oplus 0.146814$
5	$2.38231 \pm 1.5 \oplus 0.349486$
6	$0.910659 \pm 1 \oplus 0.220425$
7	$1.19564 \pm 1 \oplus 0.258476$
8	$1.59349 \pm 1.5 \oplus 0.294614$

Table 3.3: *Number of 4π vs $K_S^0\pi\pi$ background events per bin in the data sample. The first error is the Poisson error on the yields, the second error comes from the sys- tematic uncertainty on the distribution over the bins.*

3.4 Determination of number of flat and continuum background events

The total number of flat bkg events and continuum bkg events is determined using a form of the 'Powell method'.

In this method the missing mass squared region is divided into three regions: the lower region ($0.05\,GeV^2$ - $0.2\,GeV^2$), the signal region ($0.2\,GeV^2$ - $0.3\,GeV^2$) and the higher region ($0.45\,GeV^2$ - $0.8\,GeV^2$). The raw event yield D_i in rach sideband i is expressed as:

$$D_i = T_{Si} + T_{Pi} + T_{Ci} + T_{Fi} \tag{3.5}$$

where T_{Si} denotes the raw signal yield in sideband i, T_Pi the raw yields of peaking bkg events, T_Fi the raw yields of flat bkg events and T_{Ci} the raw yields of continuum events.

Since the raw peaking bkg yield has been calculated earlier, we get a system of three equations, one for each region of missing mass squared:

$$D_i - T_{Pi} = T_{Si} + T_{Ci} + T_{Si} \tag{3.6}$$

By assuming that the ratio of numbers of events in each sideband is modulated correctly by the MC samples - e.g. $T_{S1} = \frac{m_{S1}}{m_{S2}}T_{S2}$, where m_{Si} is the number of signal events in the MC sample - these three equations can be expressed in terms of three unknowns:

$$D_1 - T_{P1} = \frac{m_{S1}}{m_{S2}}T_{S2} + T_{C1} + \frac{m_{F1}}{m_{F3}}T_{F3} \tag{3.7}$$

$$D_2 - T_{P2} = T_{S2} + \frac{m_{C2}}{m_{C1}}T_{C1} + \frac{m_{F2}}{m_{F3}}T_{F3} \tag{3.8}$$

$$D_3 - T_{P3} = \frac{m_{S1}}{m_{S3}}T_{S2} + \frac{m_{C3}}{m_{C1}}T_{C1} + T_{F3} \tag{3.9}$$

This system can be solved by a simple matrix inversion and thus the number of continuum and flat bkg events in the signal window found (Chris thesis Section 3.6.3).

The difference to method described in Chris thesis is that instead of dividing the flat bkg into 'peaking in low sideband' and 'peaking in high sideband' the bkg is divided into continuum and flat bkg.

This results in 42.07 flat bkg events in the data sample and 17.06 continuum events. The continuum bkg is also assumed to be flat in phasespace, so the 17 events are distributed according to the area of the bins. This results in the following number of continuum events per bin:

bin i	B_i^{cont}
1	5.63723 ± 2.5
2	1.94538 ± 1
3	1.08944 ± 1
4	1.00759 ± 1
5	2.27215 ± 1.5
6	1.37909 ± 1.5
7	1.43683 ± 1.5
8	2.28738 ± 1.5

Table 3.4: *Number of continuum bkg events per bin in the data sample. The error is the Poisson error on the bin-yields.*

The number of flat bkg events in bin i are then:

bins	B_i^{flat}
1	13.9052 ± 4
2	4.79864 ± 2
3	2.6873 ± 1.5
4	2.4854 ± 1.5
5	5.60467 ± 2.5
6	3.40177 ± 1.5
7	3.5442 ± 1.5
8	5.64223 ± 2.5

Table 3.5: *Number of flat bkg events per bin in the data sample. The error is the Poisson error on the bin-yields.*

3.5   Determination of the signal selection-efficiency

The signal selection efficiency in each bin is determined using a sample of $50\,000$ $K_L^0 \pi \pi$ vs 4π signal MC events. The results are listed below.

bin	$\epsilon\ [\ \%]$
1	0.27805 ± 0.00155862
2	0.270163 ± 0.00262954
3	0.2553 ± 0.00345042
4	0.258504 ± 0.00360249
5	0.262955 ± 0.00241227
6	0.26856 ± 0.00311724
7	0.266931 ± 0.00304808
8	0.267617 ± 0.00241776

Table 3.6: *Signal efficiency per bin.*

3.6   Resulting MM_i

Since M_i and M_{-i} are the same, the numbers are directly evaluated for the sum of M_i and M_{-i} and listed on the table below.

bin	MM_i
1	$134.113 \pm 13.8788 \oplus 0.751773 \oplus 1.02659$
2	$59.2287 \pm 8.89065 \oplus 0.576484 \oplus 0.662635$
3	$55.3925 \pm 8.62598 \oplus 0.748637 \oplus 0.640571$
4	$20.3397 \pm 5.73716 \oplus 0.283453 \oplus 0.459255$
5	$46.0104 \pm 8.63545 \oplus 0.422086 \oplus 0.646829$
6	$24.5822 \pm 6.22456 \oplus 0.285332 \oplus 0.415563$
7	$61.1564 \pm 8.97011 \oplus 0.698343 \oplus 0.71385$
8	$84.1326 \pm 10.7023 \oplus 0.76009 \oplus 0.807176$

Table 3.7: *$M_i + M_{-i}$ The first error comes from the Poisson error on the raw data yields and the bkg yields and the second error from the systematic uncertainty on the peaking bkg distribution and the third from the signal reconstruction and selection efficiency.*

3.7   Summary

bin	raw yields	$B_i^{peak}(K_L^0\pi\pi\,vs\,K_S^0\pi\pi)$	$B_i^{peak}(K_S^0\pi\pi\,vs\,4\pi)$	B_i^{cont}	B_i^{flat}	signal
1	172	12.26	1.32	13.90	5.63	134.11
2	71	3.81	0.85	4.79	1.94	59.22
3	60	2.85	0.70	2.68	1.08	55.39
4	25	1.48	0.43	2.48	1.00	20.33
5	59	3.68	2.38	5.60	2.27	46.01
6	32	1.72	0.91	3.40	1.37	24.58
7	71	4.03	1.19	3.54	1.43	61.15
8	99	5.63	1.59	5.64	2.28	84.13

Table 3.8: *Summary of contributions to the raw yields per bin.*

4. Systematic uncertainties

4.1 Sources of systematic uncertainties

4.1.1 Non-flat flat and continuum bkg

In order to evaluate the effect of the flat and continuum bkg possibly not being flat the distribution of flat bkg events and continuum bkg events is taken from the generic MC and continuum MC respectively.

4.1.2 Peaking bkg distribution

There are different components to the systematic uncertainty from the peaking bkg distribution:

4.1.2.1 Limited data and MC sample

Uncertainty from the limited data and MC used to execute the procedure described in Section 2.3.2 and Section 3.3.
This uncertainty is calculated directly and listed with the default results in Table 2.6 and Table 3.7 for 4π vs $K_S^0\pi\pi$ and 4π vs $K_L^0\pi\pi$ respectively.

4.1.2.2 Cleanness of data sample

Uncertainty from the cleanness of the data samples used to determine the distribution of peaking bkg events where the reconstructed 4π comes from a $K_S^0\pi\pi$ decay(see Sections 2.3.2.1 and 3.3.2). The effect of this systematic is estimated by assuming that the data sample consists of 96% and 92% peaking bkg events while the rest of the events is are distributed according to the generic MC.

4.1.2.3 Unknown BR($D^0 \to K_L^0\pi\pi$)

Uncertainty in the 4π vs $K_L^0\pi\pi$ case on the total number of $K_L^0\pi\pi$ vs $K_L^0\pi\pi$ bkg events in the data sample.
This uncertainty occurs due to the extrapolation of peaking bkg events from generic MC. Since the branching fraction of D to $K_L^0\pi\pi$ is not known, this number cannot be exact. To estimate this uncertainty the number of peaking bkg events is varied by $\pm$ 20%.

4.1.3   Multiple candidate selection

A different multiple candidate selection is tested. Instead of selecting the best candidate based on $m_b c$ a candidate is chosen at random.

4.1.4   Dalitz plot acceptance

The Dalitz plot acceptance is estimated in bins of pion track momentum p and angle θ as described in Chris report.

p bin	θ bin 1	2	3	4
1	0.912 ± 0.006	1.010 ± 0.006	0.997 ± 0.006	0.976 ± 0.006
2	0.972 ± 0.006	1.060 ± 0.006	1.060 ± 0.006	1.040 ± 0.006
3	0.962 ± 0.006	1.050 ± 0.006	1.040 ± 0.006	1.030 ± 0.006
4	0.876 ± 0.008	0.984 ± 0.009	0.979 ± 0.009	0.938 ± 0.008

Table 4.1: *Normalized Dalitz plot efficiency for 4π vs $K^0_S \pi\pi$.*

p bin	θ bin 1	2	3	4
1	0.912 ± 0.005	1 ± 0.006	1.01 ± 0.005	0.976 ± 0.004
2	0.973 ± 0.004	1.06 ± 0.006	1.06 ± 0.005	1.04 ± 0.004
3	0.966 ± 0.005	1.05 ± 0.006	1.05 ± 0.005	1.03 ± 0.004
4	0.853 ± 0.006	0.967 ± 0.007	0.968 ± 0.007	0.924 ± 0.006

Table 4.2: *Normalized Dalitz plot efficiency for 4π vs $K^0_L \pi\pi$.*

4.2 Effects on the number of signal events in 4π vs $K_S^0\pi\pi$

bin i	default	4.1.1	4.1.2.2	4.1.3	4.1.4
1	$30.78 \pm 6.97 \oplus 0.24 \oplus 0.65$	31.13	30.69	29.68	28.60
2	$19.83 \pm 5.25 \oplus 0.27 \oplus 0.45$	18.64	19.79	19.44	20.29
3	$16.38 \pm 4.47 \oplus 0.27 \oplus 0.50$	16.73	16.34	15.8	15.03
4	$10.15 \pm 3.38 \oplus 0.18 \oplus 0.30$	10.63	10.16	12.30	7.96
5	$55.14 \pm 8.04 \oplus 0.68 \oplus 0.56$	54.22	55.11	50.81	54.91
6	$21.08 \pm 5.08 \oplus 0.33 \oplus 0.38$	20.29	21.11	21.98	21.47
7	$27.67 \pm 5.94 \oplus 0.43 \oplus 0.57$	28.50	27.86	27.20	29.17
8	$36.88 \pm 6.78 \oplus 0.45 \oplus 0.62$	37.73	36.82	32.06	35.99

Table 4.3: *4π vs $K_S^0\pi\pi$ efficiency corrected and bkg subtracted signal events for different systematic effects. The first error on the default values is statistical, the second one from uncertainty on the signal efficiency and the third one is the uncertainty from the limited data and MC sample used to determine the distribution of peaking bkg events(Section 4.1.2.1). The systematic effects are from left to right: non-flat bkg, peaking bkg (cleanness of data sample 96%), multiple candidate selection, Dalitz plot acceptance.*

4.3 Effects on the number of signal events in 4π vs $K_L^0\pi\pi$

bin i	default	4.1.1	4.1.2.2	4.1.2.3	4.1.2.3	4.1.3	4.1.4
1	$134.11 \pm 13.89 \oplus 0.75 \oplus 1.03$	137.64	134.13	136.48	131.73	132.90	132.8
2	$59.23 \pm 8.89 \oplus 0.58 \oplus 0.66$	61.89	59.24	59.98	58.46	60.44	62.05
3	$55.39 \pm 8.63 \oplus 0.75 \oplus 0.64$	51.45	55.36	55.99	54.78	55.04	54.40
4	$20.34 \pm 5.74 \oplus 0.28 \oplus 0.46$	20.80	20.37	20.65	20.02	18.21	19.45
5	$46.01 \pm 8.64 \oplus 0.42 \oplus 0.65$	42.58	46.04	46.76	45.25	45.15	46.96
6	$24.58 \pm 6.22 \oplus 0.29 \oplus 0.42$	26.55	24.61	24.92	24.23	24.43	24.59
7	$61.16 \pm 8.97 \oplus 0.70 \oplus 0.71$	60.00	61.11	61.97	60.34	62.27	61.44
8	$84.13 \pm 10.70 \oplus 0.76 \oplus 0.81$	84.02	84.10	85.26	82.99	83.66	85.41

Table 4.4: *4π vs $K_S^0\pi\pi$ efficiency corrected and bkg subtracted signal events for different systematic effects. The first error on the default values is statistical, the second one from uncertainty on the signal efficiency and the third one is the uncertainty from the limited data and MC sample used to determine the distribution of peaking bkg events(Section 4.1.2.1). The systematic effects are from left to right: non-flat bkg, peaking bkg (cleanness of data sample 92%), peaking bkg ($BR(D^0 \to K_L^0\pi\pi)$ 20% smaller than in genMC), peaking bkg ($BR(D^0 \to K_L^0\pi\pi)$ 20% greater than in genMC), multiple candidate selection, Dalitz plot acceptance.*

5. Fit for F_+

5.1 Fractional flavour-tagged $K^0_{\mathrm{S}}\pi\pi$ yields T_i

The given values for K'_i obtained from Table 1 of `arXiv:1210.939` contain effects from charm-mixing that cancel in our case. The factors T_i without mixing are archived by numerically solving the system of equations:

$$K'_i = T_i + \sqrt{T_i T_{-i}}(yc_i + xs_i) \qquad (5.1)$$

where x and y charm-mixing parameters. The fit also takes into account that the sum over the T_i should be one by fixing $T_1 = 1 - \sum_{i \neq 1} T_i$. The values for x and y are take from the latest HFAG results ($x = (0.63 \pm 0.19)\%$, $y = (0.75 \pm 0.12)\%$) and the values for c_i and s_i are taken from `arXiv:1010.2817`. In the fit all input variables are Gaussian constraint and the correlation between c_i and s_i are taken into account. The resulting T_i are listed below.

bin	T_i	bin	T_i
1	0.1695 ± 0.0053	-1	0.0781 ± 0.0014
2	0.0873 ± 0.0012	-2	0.0186 ± 0.0002
3	0.0723 ± 0.0020	-3	0.0201 ± 0.0003
4	0.0258 ± 0.0011	-4	0.0161 ± 0.0015
5	0.0889 ± 0.0024	-5	0.0523 ± 0.0013
6	0.0589 ± 0.0011	-6	0.0147 ± 0.0003
7	0.1252 ± 0.0018	-7	0.0132 ± 0.0004
8	0.1320 ± 0.0021	-8	0.0270 ± 0.0010

Table 5.1: *Fraction flavour-tagged $K^0_{\mathrm{S}}\pi\pi$ yields without mixing-effects.*

5.2   Fractional flavour-tagged $K_L^0\pi\pi$ yields T_i'

The fractional flavour-tagged $K_L^0\pi\pi$ yields are taken from Sean Brisbane's thesis (Section 3., Table 3.14). They are listed below:

bin	T_i'	bin	T_i'
1	0.163 ± 0.004	-1	0.090 ± 0.017
2	0.069 ± 0.003	-2	0.024 ± 0.005
3	0.061 ± 0.003	-3	0.031 ± 0.006
4	0.026 ± 0.002	-4	0.019 ± 0.004
5	0.082 ± 0.003	-5	0.057 ± 0.014
6	0.058 ± 0.002	-6	0.017 ± 0.004
7	0.122 ± 0.003	-7	0.021 ± 0.003
8	0.124 ± 0.003	-8	0.035 ± 0.008

Table 5.2: *Fraction flavour-tagged $K_L^0\pi\pi$ yields.*

5.3   Results F_+

A fit for F_+ is performed for the default signal results, for the results with stat. error only, and for each systematic effect listed in Chapter 4. The error from the systematic error from the signal selection and reconstruction efficiency and the limited data and MC sample used to determine the peaking bkg distributions (those were determined alongside the statistical error) are determined by comparing the fit results with stat. error only and stat. error $\oplus$ sys. error.

Listing the statistical error and the systematic error from the Dalitz plot acceptance separately this results in $F_+ = 0.7372 \pm 0.0510 \pm 0.0103 \pm 0.0083$.
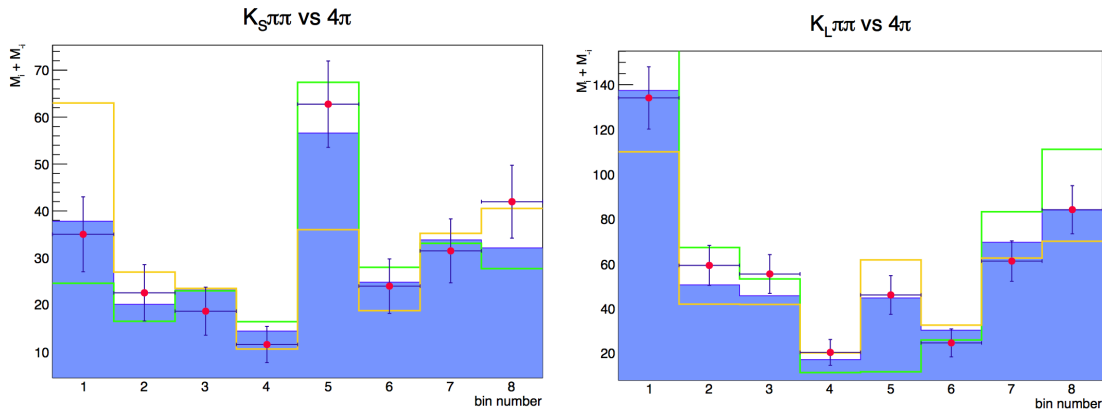

Figure 5.1: *Distribution of signal yields per bin for $K_S^0\pi\pi$ (left) and $K_L^0\pi\pi$ (right). Red: data, blue histogram: fit results (fit to $K_S^0\pi\pi$ and $K_L^0\pi\pi$ separately), orange: values for F_+=0.5, green: values for F_+=1.0.*
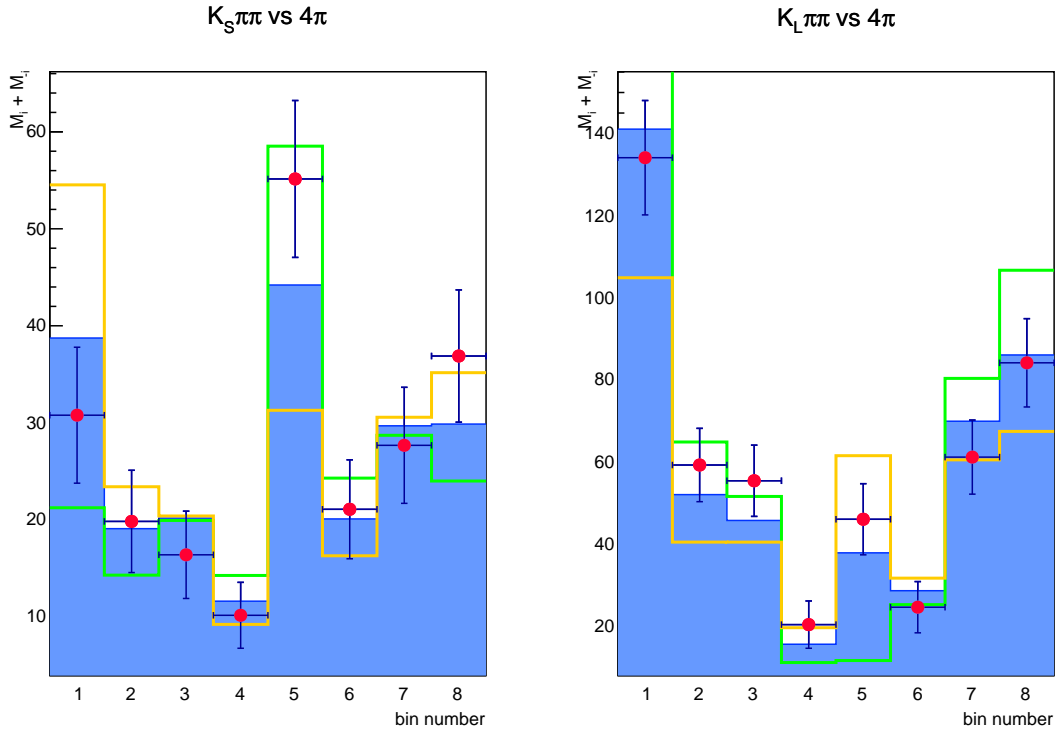
Figure 5.2: *Distribution of signal yields per bin for $K_S^0\pi\pi$ (left) and $K_L^0\pi\pi$ (right). Red: data, blue histogram: fit results (fit to $K_S^0\pi\pi$ and $K_L^0\pi\pi$ simultaneously), orange: values for $F_+=0.5$, green: values for $F_+=1.0$.*

	$K_S^0\pi\pi$ Fit	$K_L^0\pi\pi$ Fit	sim. Fit
default	$\mathbf{F_+^{K_S^0\pi\pi} = 0.828 \pm 0.075}$ $h_{norm}^{K_S^0\pi\pi} = 111.9 \pm 8.88$ $\chi^2_{ndof} = 0.64$	$\mathbf{F_+^{K_L^0\pi\pi} = 0.67 \pm 0.064}$ $h_{norm}^{K_L^0\pi\pi} = 220.19 \pm 15.01$ $\chi^2_{ndof} = 0.72$	$\mathbf{F_+^{sim} = 0.7372 \pm 0.0510}$ $h_{norm}^{K_S^0\pi\pi} = 110.49 \pm 8.83$ $h_{norm}^{K_L^0\pi\pi} = 213.11 \pm 14.41$ $\chi^2_{ndof} = 0.40$
stat. only	$F_+^{K_S^0\pi\pi} = 0.828 \pm 0.075$ $h_{norm}^{K_S^0\pi\pi} = 111.9 \pm 8.82$ $\chi^2_{ndof} = 0.64$	$F_+^{K_L^0\pi\pi} = 0.670 \pm 0.064$ $h_{norm}^{K_L^0\pi\pi} = 220.14 \pm 14.95$ $\chi^2_{ndof} = 0.72$	$F_+^{sim} = 0.7374 \pm 0.0508$ $h_{norm}^{K_S^0\pi\pi} = 110.48 \pm 8.78$ $h_{norm}^{K_L^0\pi\pi} = 213.11 \pm 14.35$ $\chi^2_{ndof} = 0.41$
flat bkg	$F_+^{K_S^0\pi\pi} = 0.823 \pm 0.073$ $h_{norm}^{K_S^0\pi\pi} = 112.01 \pm 8.69$ $\chi^2_{ndof} = 0.61$	$F_+^{K_L^0\pi\pi} = 0.689 \pm 0.062$ $h_{norm}^{K_L^0\pi\pi} = 218.19 \pm 14.40$ $\chi^2_{ndof} = 0.68$	$F_+^{sim} = 0.7456 \pm 0.0490$ $h_{norm}^{K_S^0\pi\pi} = 110.75 \pm 8.64$ $h_{norm}^{K_L^0\pi\pi} = 212.36 \pm 13.84$ $\chi^2_{ndof} = 0.37$
peak clean	$F_+^{K_S^0\pi\pi} = 0.829 \pm 0.075$ $h_{norm}^{K_S^0\pi\pi} = 111.87 \pm 8.83$ $\chi^2_{ndof} = 0.63$	$F_+^{K_L^0\pi\pi} = 0.670 \pm 0.064$ $h_{norm}^{K_L^0\pi\pi} = 220.24 \pm 15.01$ $\chi^2_{ndof} = 0.72$	$F_+^{sim} = 0.7375 \pm 0.0510$ $h_{norm}^{K_S^0\pi\pi} = 110.49 \pm 8.78$ $h_{norm}^{K_L^0\pi\pi} = 213.08 \pm 14.41$ $\chi^2_{ndof} = 0.40$
0.8·BR($K_L^0\pi\pi$) 4.1.2.3	$F_+^{K_S^0\pi\pi} = 0.828 \pm 0.075$ $h_{norm}^{K_S^0\pi\pi} = 111.9 \pm 8.88$ $\chi^2_{ndof} = 0.64$	$F_+^{K_L^0\pi\pi} = 0.669 \pm 0.063$ $h_{norm}^{K_L^0\pi\pi} = 223.55 \pm 14.99$ $\chi^2_{ndof} = 0.73$	$F_+^{sim} = 0.7356 \pm 0.0505$ $h_{norm}^{K_S^0\pi\pi} = 110.44 \pm 8.83$ $h_{norm}^{K_L^0\pi\pi} = 216.53 \pm 14.41$ $\chi^2_{ndof} = 0.41$
1.2·BR($K_L^0\pi\pi$) 4.1.2.3	$F_+^{K_S^0\pi\pi} = 0.828 \pm 0.075$ $h_{norm}^{K_S^0\pi\pi} = 111.9 \pm 8.88$ $\chi^2_{ndof} = 0.64$	$F_+^{K_L^0\pi\pi} = 0.671 \pm 0.065$ $h_{norm}^{K_L^0\pi\pi} = 216.81 \pm 15.03$ $\chi^2_{ndof} = 0.71$	$F_+^{sim} = 0.7396 \pm 0.0520$ $h_{norm}^{K_S^0\pi\pi} = 110.55 \pm 8.83$ $h_{norm}^{K_L^0\pi\pi} = 209.67 \pm 14.41$ $\chi^2_{ndof} = 0.40$
mult. can.d sel.	$F_+^{K_S^0\pi\pi} = 0.8351 \pm 0.0777$ $h_{norm}^{K_S^0\pi\pi} = 110 \pm 8.96$ $\chi^2_{ndof} = 0.41$	$F_+^{K_L^0\pi\pi} = 0.6751 \pm 0.0640$ $h_{norm}^{K_L^0\pi\pi} = 220.11 \pm 15.00$ $\chi^2_{ndof} = 0.59$	$F_+^{sim} = 0.7406 \pm 0.0516$ $h_{norm}^{K_S^0\pi\pi} = 108.84 \pm 8.93$ $h_{norm}^{K_L^0\pi\pi} = 213.32 \pm 14.45$ $\chi^2_{ndof} = 0.30$
Dalitz acceptance	$F_+^{K_S^0\pi\pi} = 0.831 \pm 0.079$ $h_{norm}^{K_S^0\pi\pi} = 108.77 \pm 9.05$ $\chi^2_{ndof} = 0.92$	$F_+^{K_L^0\pi\pi} = 0.669 \pm 0.064$ $h_{norm}^{K_L^0\pi\pi} = 221.53 \pm 15.30$ $\chi^2_{ndof} = 0.72$	$F_+^{sim} = 0.7349 \pm 0.0522$ $h_{norm}^{K_S^0\pi\pi} = 107.44 \pm 9.00$ $h_{norm}^{K_L^0\pi\pi} = 214.58 \pm 14.75$ $\chi^2_{ndof} = 0.54$
c_i etc. fixed	$F_+^{K_S^0\pi\pi} = 0.828 \pm 0.074$ $h_{norm}^{K_S^0\pi\pi} = 111.77 \pm 8.69$ $\chi^2_{ndof} = 0.65$	$F_+^{K_L^0\pi\pi} = 0.666 \pm 0.057$ $h_{norm}^{K_L^0\pi\pi} = 220.18 \pm 13.75$ $\chi^2_{ndof} = 0.91$	$F_+^{sim} = 0.7289 \pm 0.0494$ $h_{norm}^{K_S^0\pi\pi} = 110.05 \pm 8.71$ $h_{norm}^{K_L^0\pi\pi} = 212.5 \pm 13.44$ $\chi^2_{ndof} = 0.43$

Table 5.3: *Fit results for the default signal yields and the signal yields with systematic effects.*

source	uncertainty
stat. error	$\pm$ 0.0510
sys. error	$\pm$ 0.0045
non-flat bkg	$\pm$ 0.0084
peak bkg clean.	$\pm$ 0.0003
diff. BR($K_\mathrm{L}^0\pi\pi$)	$\pm_{0.0016}^{0.0024} \approx \pm$ 0.002
mult. cand. sel.	$\pm$ 0.0034
Dalitz acceptance	$\pm$ 0.0083

Table 5.4: *Uncertainties on the value of F_+ from different sources.*